Manipulating Deformable Linear Objects: Sensor-Based Skills of Adjustment Motions for Vibration Reduction

***Shigang YUE and **Dominik HENRICH**

*Ridley Building, School of Biology, University of Newcastle, Newcastle upon Tyne NE1 7RU, UK
**Robotics and Embedded Systems, Applied Computer Science III, University of Bayreuth 95440 Bayreuth, GERMANY
E-Mail: shigang.yue@ncl.ac.uk, and dominik.henrich@uni-bayreuth.de

Abstract: *The vibration of a deformable object is often a problem when it is automatically handled by a robot manipulator. However, humans can often handle and damp the vibration of deformable objects with ease. This paper presents force/torque sensor-based skills for handling deformable linear objects in a manner suitable to reduce acute vibration with simple human skill inspired strategies, that consist of one or two adjustment motions. The adjustment motion is a simple open-loop motion that can be attached to the end of any arbitrary end-effector's trajectory. As an ordinary industrial robot's simple action, it has three periods, i.e., acceleration, constant speed and deceleration periods; it starts from a predicted time tightly close to a force/moment maximum. The predicted time for the adjustment action is generated automatically on-line based on the vibration rhythm and the data sensed by a force/torque sensor mounted on the robot's wrist. To find the matching point between the vibrational signal of the deformable object and a template, template matching techniques including cross-correlation and minimum squared error methods are used and compared. Experiments are conducted with an industrial robot to test the new skills under various conditions. The results demonstrate that an industrial robot could perform effective vibration reduction skills with simple strategies.*

Keywords: *deformable object, vibration reduction, skill, adjustment motions, force/torque sensor, template matching, cross-correlation, minimum squared error*

1. Introduction

Automated handling and assembly of objects have been studied by many researchers in the areas of manufacturing, robotics, and artificial intelligence. Until now, most studies assumed that the objects to be manipulated were rigid. However, deformable objects such as cables, wires, ropes, cloths, rubber tubes, sheet metals, paper sheets and leather products are common in the real world. In most cases, deformable objects and parts are still handled and assembled by humans. Practical methods for the automatic handling and manipulation of deformable objects are urgently needed. In this paper, we concentrate on deformable linear objects (DLOs), such as ropes, hoses, electric wires or leaf springs, which can be found in many industrial products.

Recent reviews of robot manipulation of deformable objects are provided by Henrich and Wörn [1] and Nakazawa [2]. Compared to the assembly of rigid workpieces, some additional aspects must be taken into consideration. The shape of the workpiece to be assembled is typically neither exactly known nor constant for the assembly process. While the initial shape depends on the history of the workpiece, the

deformation in the assembly process depends on contact forces and gravity. In addition, non-rigid workpieces have an inherent compliance which can hardly be influenced. Altogether, these effects cause high uncertainties that have to be dealt with.

There are two principle ways to cope with these problems. On the one hand, the behavior of the workpiece may be taken into account by means of a quantitative deformation model for computing the shape of the workpiece. On the other hand, the deformation can be regarded as uncertainty that must be sensed and/or compensated for while performing the assembly.

The use of deformation models for handing DLOs has been investigated by several researchers; for example, Zheng et al. determined the required gripper trajectory for inserting a flexible beam into a rigid hole by computing the deflection curve of the beam [3], Wakamatsu et al. presented a general algorithm for computing the shape of elastic DLOs [4] and Hirai et. al. modeled the deformable objects for simulation considering bend, twist, and extension in 3D space [5]. These methods can be used if all relevant parameters, geometries and boundary conditions are exactly known. Without additional sensor information, they are likely to fail in the presence of uncertainties.

Other works are based on sensor integration. Inoue and Inaba used a stereo vision system for picking-up a rope and guiding it through a ring [6], Smith et. al. conducted vision-based manipulation of non-rigid objects [7], while others inserted bending beams into holes under friction (Kraus and McCarragher [8] with force-based approach, Nakagaki et al. [9] with vision-based approach). All of those approaches are used for solving clearly specified tasks, but it is not clear how they may be re-used in other, similar situations.

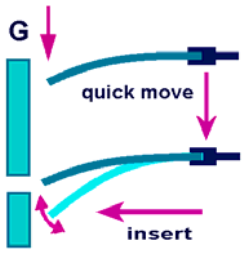

Figure 1. The vibration caused by a quick operation results in uncertainty and failure, e.g., when inserting a DLO into a hole in a gravity field

When a robot executes a manipulation task, its motion can be divided into several motion primitives, each of which has a particular target state to be achieved in the task context. These primitives are called ‘skills’. An adequately defined skill can have generality to be applied to various similar tasks. Until now, most of the research work on skill-based manipulation deals with rigid objects [10-12].

Skill-based manipulation for handling deformable linear materials has been touched upon recently. For example, Henrich et. al [13] analyzed the contact states and point contacts of DLOs with regard to manipulation skills, Abegg et. al [14] studied the

contact state transitions based on force and vision sensors and Remde et.al [15] discussed the problem of picking-up DLOs by experimentation.

However, the effects of vibration are not taken into account in the skill-related work described above. The dynamic effects of deformable objects cannot be neglected, especially when the objects are moved quickly by a robot arm. As shown in Figure 1, the uncertainty resulting from oscillation may cause failure during the insert-into-hole operation. Therefore, the vibration caused by inertia should be depressed during the motion or eliminated as soon as possible after the motion.

Vibration reduction of flexible structures has been a research topic for many researchers, and Chen et al. have reviewed the previous works [16]. Chen et al. also present a passive approach based on an open-loop concept for vibration-free handling of deformable beams; similar ideas can be found in [17,18], which applied the 'input shaping' using a robot [18] but dealt only with rigid bodies. However, application of the method presented by [16] is limited due to its stable start condition of the robot motion and a relatively simple trajectory of the previous motion. Considering the complex manipulations involved in practical situations, such as avoiding obstacles, picking-up and insert-into-hole, stable start condition cannot be satisfied easily.

With respect to manipulation, only the vibration that may cause failure of the next operation must be eliminated. Therefore, we prefer to remove as much as possible of the unwanted vibration immediately after the previous motion. *Previous motion* here refers to motions that are completed before the next operation starts and result in vibration in the DLO. In a recent paper, we discussed a model-based method to reduce the vibration of DLOs using attachable adjustment motions [19]. Although the model-based method has proved the effectiveness of the adjustment motion, it is computed off-line. Moreover, it depends on how well the model matches the real DLOs, and how well the simulated robot operation matches the real robot operation. These disadvantages are general and hold true for all model-based approaches.

To overcome these disadvantages, we present sensor-based skills to eliminate acute vibration of DLOs on-line. With the new skills, no model is needed to describe DLO's dynamic behaviors; the status of the DLO is recognized by analyzing on-line data from sensors. Visual sensors are not considered here for their low sampling rate (usually less than 25Hz, or at every 40ms) and high computing cost. Data from a force/torque sensor (sampling rate is as high as 62.5Hz, or at every 16ms) mounted on the wrist of the robot is employed to find the actual status of the DLO by using template matching methods.

The idea of the sensor-based adjustment motion is based on observations of human skills. For example, holding a long stainless steel ruler as a DLO, even only with translation movements, we could start our effective vibration reduction by adjusting our hand position within a very limited space and time. The area needed, the acceleration and the speed of the hand and the time to start the adjustment motion are correlated in human skill. One may argue that a human hand can always deliver more delicate acceleration profiles than any industrial robot. This is probably true. However, whether these delicate accelerations are needed for a human to fulfill these skills remains unknown. In the paper, we will show that an industrial robot, with a force/torque sensor and limited types of acceleration profiles, can also conduct a very effective skill to reduce acute vibration of DLOs.

The vibration reduction skill presented in this paper is an open-loop skill and it does not involve any feedback-based control law or any change of the acceleration profiles developed by robot suppliers and illustrated in detail in the robot manuals. Therefore, it could be easily used in practice in similar situations.

The rest of this paper consists of five parts. The strategies are discussed and specified in Section 2. The template matching methods used to determine the main parameters of the vibration signal are described in Section 3. Implementation of the experiments is given in Section 4. Experimental results validating the effectiveness of the proposed sensor-based manipulating skill are shown in Section 5. Finally, conclusions and future work are related.

2. Strategies

With the force/torque sensor mounted on the wrist of the robot, the vibrational pattern and other critical parameters can be known before skills are conducted. Therefore, no accurate model is needed. The most important thing is to determine when to start the adjustment motion and how to adjust to the known vibration strength and pattern of the DLO. However, some illustrations and assumptions are still listed here for a better understanding of our strategy design.

2.1 Vibration patterns

2.1.1 Residual vibration period

Since only the vibration that may cause failure of the next operation should be eliminated, adjustment motion can be done during the residual period immediately after the corresponding previous motion. There is no externally exciting force during this residual vibration period, so the vibration of DLOs is a kind of *free vibration* without excited force. A DLO may have many modes of vibration. However, in most cases, the dominant vibration is governed mainly by the first mode. To simplify the description, we use a one degree-of-freedom (DOF) system as an example. It is also assumed that the DLO behaves like a linear spring with constant stiffness. Thus, we have the following equations for *free vibration* [20],

$$m\ddot{x} + c\dot{x} + kx = 0 \tag{1}$$

where x is the endpoint displacement, m is the mass, c is the damping coefficient, and k is the stiffness of the spring. The solution of equation (1) is as follows when the damping is light;

$$x = Ae^{-\alpha t}\sin(\omega t + \eta) \tag{2}$$

where A and η depend upon initial conditions, $\alpha = c/2m$ and ω is the frequency of oscillation. Equation (2) describes the residual vibrational displacement of a one DOF system, implying that the vibration of such a DLO behaves like a Sine function.

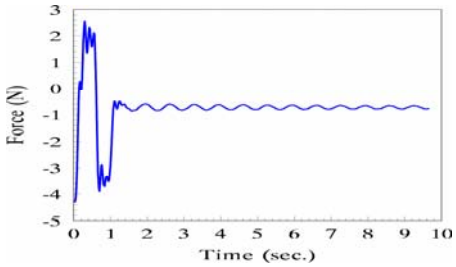

Figure 2. A typical low-pass filtered force signal of a DLO F_y during previous motion (0 to 1 sec.) and residual period (after 1 sec.). It behaves most like Sine wave though the DLO has more than one flexible DOF.

The force or moment signals are also Sine functions, according to the solution. A typical DLO's force signal obtained using a force/torque sensor is shown in Figure 2. It behaves most like Sine functions too, although in fact the DLO may have more than one flexible DOF. Therefore, it is reasonable to employ standard Sine functions as templates for comparison with signals from the sensor during residual vibration periods. However, if a DLO behaves in a different way, other kinds of template might be used.

2.1.2 Vibration during handling

If the free vibrating DLO is handled with various accelerations and speeds, the vibration will be increased or decreased. During the acceleration and deceleration period, the DLO is in fact excited by external forces. In this situation, the vibration of the DLO can be treated as *forced vibration*.

The damped forced vibration equation can be written as [20]:

$$m\ddot{x} + c\dot{x} + kx = F\sin(\omega_1 t) \tag{3}$$

if the exciting force is periodical.

It is well-known that if the excitation frequency of the system ω_1 happens to coincide with the natural frequency of the system ω , i.e., when ω_1/ω=1, the dynamic magnification reaches very high values, although these are attenuated by the damping present. The frequency at which the peak dynamic magnification occurs is called the *resonance frequency*.

On the other hand, for an already existing free vibration, if an opposite phase exciting force with the same resonance frequency is added for a short time for example, the vibrational amplitude will be reduced. Therefore, in our strategy design, we will make use of resonance frequency to increase the skill's efficiency. Vibration reduction without considering resonance frequency might also be possible but is not the topic of this paper.

In this paper, the dominant natural frequency ω (or vibrational period T) and the stiffness of the DLO are measured experimentally with the force/torque sensor and used as known parameters when manipulating a certain DLO.

2.2 Basic Strategy

Here **Adjustment motion** refers to a kind of open-loop small-scale motion that can be performed by a robot end-effector (or jaws in this paper) after any arbitrary trajectory to damp the vibration caused by this previous motion. Most of the possible adjustment motions can be sorted into two different groups according to the type of motion involved [19]. One is translation-adjustment motion (TAMo) and another is rotation-adjustment motion (RAMo). The adjustment motions can also be classified as one-way adjustment motion and two-way adjustment motion, as shown in Figure 3. Two-way adjustment-motion style is very convenient for the immediate execution of the next operation because the robot's jaws are back to their original position. Unlike model-based methods, the sensor-based adjustment motion will be generated on-line and automatically according to the results of vibrational data analysis. The style of adjustment motion used here is TAMo.

DSA (distance, speed and acceleration profiles): An adjustment motion could be defined by specifying its acceleration, speed, deceleration and distance precisely. However, an industrial robot can perform only limited types of acceleration profiles. We have to define the adjustment motion in a simplified way: define it with distance, speed and acceleration profiles. In other words, with the combined speed and acceleration profiles, we hope that the robot jaws are able to cover a short distance within a certain period of time with one type of acceleration profile. DSA specifies the flexible pattern of adjustment motion. For example, we want the robot end-effector to run along a straight line for 25cm within 0.25sec with acceleration profile type 1. This would mean its speed should reach 1m/s at least; this seems easy for an industrial robot whose highest speed may be over 5m/s.

The basic strategy: The basic strategy of the sensor-based skill consists of not only the DSA of the adjustment motion, but also the time (when the robot jaws start the adjustment motion) and the direction (which direction the robot jaws should move to). To reduce the vibration of a DLO, one of the strategies of human skill is to try to prevent the DLO from regaining elastic energy once the adjustment begins, though a subject can almost start his hand at any time regardless of the current status of the DLO. The ongoing adjustment motion's accelerations, speed and scope are deeply correlated with the start time and direction in the human skill. In our strategy design, the vibrational period and strength of the DLO can be reflected with the flexible DSA. Once the time and direction of the adjustment motion are determined, the DSA are able to be formed in a way that the DLO's vibrational amplitude will shape the distance of the robot jaws' adjustment motion, and the vibrational period, together with the amplitude, will shape the speed and acceleration profiles of the robot jaws.

Time to start: to reduce the DLO's vibration, humans often start from one of the extreme positions, when the DLO is deflected to either its left or right extreme. The reason is probably because at the two extreme positions, the speed of the deflection is the lowest and is easily tracked with the eyes. Similarly, we chose to start our robot adjustment motion when moment/force reaches one of its maximum or minimum values. Actually, often the robot could not start exactly at the time we expected due to computing error and internal system delay. However, these perturbations could not affect the skill very much if they were far less than the DLO's vibrational period. To start the adjustment motion from other non-maximum or non-minimum points might be

possible (as observed in human skills) but should be accompanied by other correlated DSA.

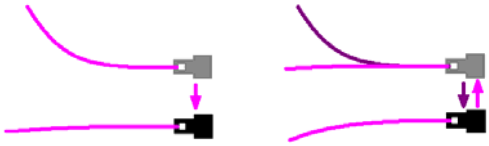

(a) (b)

Figure 3. The two types of adjustment motions used to build up the vibration reduction skills in our experiments. Both of the adjustment motions start from a force/moment maximum/minimum but with different DSA. (a) One-way TAMo, robot jaws will shift distance D_{one} to another position, and (b) Two-way TAMo, robot jaws will shift distance $D_{two} = 0.5D_{one}$ and return to its original position, is thought to be convenient for next operation.

Direction: there are two opposite directions for the adjustment motion to choose: follow the DLO's endpoint movement or against it. Here we chose to follow the endpoint back to its balanced position.

As related above, the robot arm will start its vibration reduction skill from one of the DLO's extreme positions (the DLO's displacement, force and moment reach their extreme at the same time) and follow the endpoint's movement back to its balanced position. The DSA of the adjustment motion will be shaped by the known vibrational period and the on-line data which reflects DLO's vibrational amplitude. However, one-way and two-way adjustment motion has different DSA.

2.3 One-way TAMo

A one-way adjustment motion consists of three parts, i.e. an acceleration period, a constant velocity period and a deceleration period. The strategy of the one-way adjustment motion is: (1) start at the time which could make the main acceleration period tightly close to the maxima area of the sensed force/moment; (2) move to follow the DLO's endpoint movement; (3) along a straight line cover a distance which equals the DLO's adjacent maximal displacement; (4) the speed and acceleration profiles should assure the whole adjustment motion is finished within a half DLO's vibrational period. The direction of the endpoint movement will be sensed by the force/torque sensor. The strategy is also illustrated in Figure 4.

According to the strategy, the entire adjustment motion period is a half vibrational period T. These maxima of the force/moment occur when

$$\sin(\omega t + \eta) = 1 \tag{4}$$

i.e. when

$$\omega t = \frac{4n+1}{2}\pi - \eta \ , \qquad (t > 0, \ \ n = 0, 1, 2, \cdots) \tag{5a}$$

The equation (5) implies a theoretically infinite number of opportunities to implement the sensor-based adjustment motion, if damping is neglected. Considering the internal delay of the robot system, the time to start the one-way adjustment motion should be modified,

$$t = \frac{1}{\omega}\left(\frac{4n+1}{2}\pi - \eta\right) - t_{sys}, \qquad (t > 0,\ n = 0,1,2,\cdots) \tag{5b}$$

where the t_{sys} is the robot system delay which highly depends on the type of robot used and is assumed as a constant for each execution.

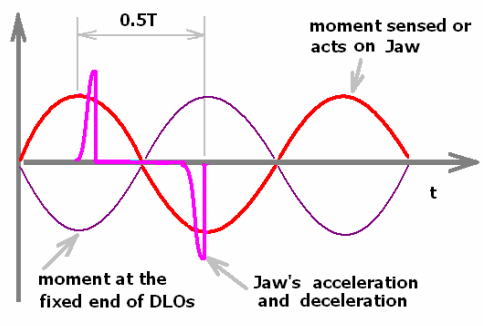

Figure 4. The sensor-based one-way adjustment motion strategy, where the Sine wave represents the sensed force/moment from the DLO and schematic acceleration profile is illustrated in pink line with impulse like shapes. The adjustment motion is expect to cover a distance equal to the vibration displacement amplitude within a half vibrational period.

The scope of the adjustment motion is determined by the vibrational amplitude of the DLO, i.e. we have the following equation;

$$s_{tamo} = \frac{1}{2}\beta f_{end} \tag{6}$$

where s_{tamo} is the distance from the start to the end of an adjustment motion, β is the damping coefficient that varies with respect to vibrational period, f_{end} is the vibrational amplitude of the DLO during the residual period and defined as the value of a maximum minus the value of an adjacent minimum.

The vibrational amplitude is known indirectly, based on the following linear stiffness assumption;

$$\delta = |f_{end}| / |M_{amp}| \tag{7}$$

where δ is a constant that can be measured in advance and M_{amp} is the amplitude of moment that can be measured on-line for each adjustment motion. The constant δ is obtained by measuring f_{end} and M_{amp} before the skill is implemented in the experiments. Here we used moment instead of force to estimate the vibrational amplitude of the DLO because moment has larger and clearer peaks and valleys, especially during acceleration

or deceleration periods, thus making feature recognition easier. However, using force does not result in vital error but less accuracy.

2.4 Two-way TAMo

Two-way adjustment motions are more practical than one-way ones. If a two-way adjustment motion is conducted, the robot jaws will finally return to the original position with the pre-adjustment posture. This characteristic of the two-way adjustment motion is more convenient for the following operation. For example, when a robot arm moves a DLO quickly from somewhere to the front of a hole (as shown in Figure 1) and is trying to insert the DLO into the hole, acute vibration caused by the quick motion may result in failure or damage. To fulfill the task efficiently, a two-way TAMo to reduce vibration followed by insertion should be one of the best choices.

A two-way adjustment motion can be defined as two tightly connected symmetrical parts, as shown in Figure 5, with each part a one-way adjustment motion. One may realize that a two-way adjustment motion and a one-way adjustment motion have almost the same strategy. The detailed strategy of a two-way adjustment motion may be described as: (1) start at the time which could cause the main acceleration impulse occur tightly close to the maxima area of the sensed force/moment; second segment starts at the time which could let the main deceleration occur tightly close to the minima area of the sensed force/moment; (2) move to follow the DLO's endpoint movement direction, which is sensed by the force/torque sensor; (3) the first segment covers a distance which equals to half of the maximal displacement, and so does the second segment; (4) the combination of speed and acceleration profiles should let the first and second segments be finished within a half DLO's vibrational period respectively.

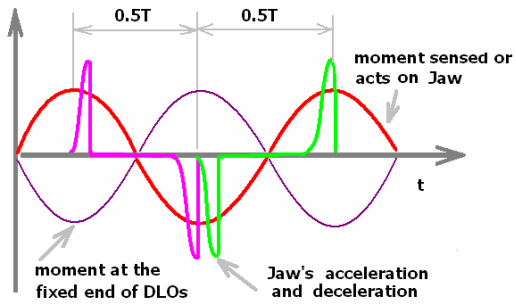

Figure 5. The sensor-based two-way adjustment motion strategy could let the robot's end-effector go back to its original position. The Sine wave represents the sensed force/moment from the DLO and the schematic acceleration profile is illustrated in pink (first part) and green (second part) lines with impulse like shapes. The two acceleration profiles are connected immediately one after another. The whole skill consists of two adjustment motions could be finished within one vibration period.

Now, the problem is, how can we find the correct time for starting the adjustment motion with only the force/torque sensor? In the following section, a template-matching method will be employed to solve this problem.

3. Sensor Data Processing

From Section 2, we learnt that the DLO's vibrational displacement theoretically behaves like a Sine function if it has one DOF. The DLO's vibration has been found to behave most like a Sine wave even with multiple flexible DOFs. We also could have sample data obtained from the sensor. If we find the *matching point* where the sample data matches the Sine function, we may use the Sine function to predict all the maxima of the vibrational signal in advance. The adjustment motion can then start based on the calculated time corresponding to one of the predicted maxima.

To find out the maximum of the vibration (sensed force/moment), the signals from the sensor will be compared with templates using different template matching techniques. Cross-correlation and minimum squared error methods will be employed to find out the match points between the signal and the template.

The sensor can provide 6D data, i.e. 3D for forces and 3D for moments. Here, only moments are used to sense the vibration of DLO. The direction of adjustment motions can be determined according to

$$\mathrm{M} = (M_x \quad M_y \quad M_z)\begin{pmatrix} i \\ j \\ k \end{pmatrix} \tag{8}$$

where $\boldsymbol{M}$ is the vector of moment and M_x, M_y and M_z are the moment in x, y and z axis, and i, j and k are the unit vectors in x, y and z axis respectively. The absolute value of the moment signal can be obtained as:

$$\|M\| = \sqrt{M_x^2 + M_y^2 + M_z^2} \tag{9}$$

Thus, the 3D data from the sensor is translated to one column and compared with the template in the following sub sections.

3.1 Cross-correlation (CCR) method

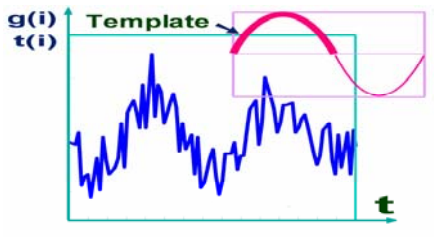

Figure 6. To recognize the matching point of the vibrational signal, a piece of the periodic signal from the sensor is compared with the template of Sine segments using the Cross-correlation (CCR) method. The signal is drawn using raw data without smoothing.

The template matching method [21] is used here to find the matching point between the signals obtained directly from the sensor and the Sine function. In fact, this is a two dimensional problem, but to save processing time, we tried to transform it into a one dimensional problem by computing the offset as described later. Let;

$g(i)$ be the signal from the sensor data
$t(i)$ be the template, and let
D be the domain of definition for the template *t(i)*.

We are looking for a region of the signal in which the signal function is similar to a previously specified template function. To measure how well a portion of the signal matches the template, the *cross-correlation* $R_{g,t}(m)$ between the two functions *g(i)* and *t(i)* is defined as;

$$R_{g,t}(m) = \sum_{i-m \in D} g(i)\ t(i-m) \tag{10}$$

Notice that this definition amounts to translating the template *t(i)* to position *(m)* in the signal. The template and the signal are declared similar when the cross-correlation is large. The normalized cross-correlation $N_{g,t}(m)$ is given by;

$$N_{g,t}(m) = \frac{1}{\sqrt{\sum_i g^2(i)}} R_{g,t}(m) \tag{11}$$

Hence, the normalized cross-correlation has a maximum value when the match with the signal function is perfect (up to a scale factor). The above definition can also be written as the following form if equation (9) is combined;

$$N_{g,t}(m) = \frac{1}{\sqrt{\sum_i (g_x^2(i) + g_y^2(i) + g_z^2(i))}} R_{g,t}(m) \tag{12}$$

A half period of Sine function with a unit amplitude is used as a template (as shown in Figure 6) and compared with each part of the digital signal obtained from the force/torque sensor, according to equation (12). The point with the largest value of $N_{g,t}$ is the matching point. The time corresponding to the maximum of $N_{g,t}$ is a *critical time*, at which displacement is a maximum. Fortunately, there are many opportunities where signal maxima are reached according to equation (5). As mentioned above, the signal data should be translated by;

$$g(i) = g(i) - g_{av} \tag{13}$$

where g_{av} is the average value of the signal within one vibration period.

3.2 Minimum squared error (MSE) method

In the above CCR method, samples should cover at least one-and-a-half periods to achieve a high success rate. We have to wait while sampling, which is very time consuming. To decrease the total time of the adjustment motion process, the sampling

time should be reduced. It is possible to find the matching point using only part of the periodic signal from the sensor, if it is carefully compared. In this case, as shown in Figure 7 for example, we used the minimum-squared-error (MSE) method to find the matching points.

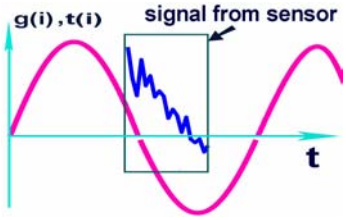

Figure 7. To recognize the matching point of the vibrational signal, a piece of the periodic signal from the sensor is compared with the template of Sine segments using the minimum squared error (MSE) method. The raw signal data from sensor may not cover a whole vibrational period.

Since the signal from the sensor does not cover even one period, it is impossible to know the offset values of the signal due to asymmetry. Therefore, sample data from the sensor should be translated in order to transfer the 2D template matching problem to a 1D one, as we do with the CCR method. Data *g(i)* from the sensor can be translated to the domain of [0,1] by,

$$g(i) = \frac{g(i) - g_{\min}}{g_{\max} - g_{\min}} \tag{14}$$

where

$$g_{\min} = \min(g(i))_{i \in D_g} \tag{15}$$

and

$$g_{\max} = \max(g(i))_{i \in D_g} \tag{16}$$

where D_s is the domain of the signal segment for comparison. The compared portion of the template can also be translated to the domain of [0,1] in the same way,

$$t(i) = \frac{t(i) - t_{\min}}{t_{\max} - t_{\min}} \tag{17}$$

where

$$t_{\min} = \min(t(i))_{i \in D_t} \tag{18}$$

and

$$t_{\max} = \max(t(i))_{i \in D_t} \tag{19}$$

where D_t is the domain of the compared portion of the template.

Now, the MSE based on the above equations (14) and (17) can be written as;

$$M_{se}(m) = \sum_{(i-m)\in D_g} (g(i-m) - t(i))^2 \tag{20}$$

Notice that it is the sensor data that is translated to the position m in this case. The definition in (20) is also the standard Euclidean distance between two vectors. The point with the smallest value of M_{se} is the matching point. By knowing the location of the matching point on the template, the time corresponding to the start point of the template can be known. Hence, the *critical times* at which displacement is at maximum or minimum can be predicted.

As we know, the vibrational amplitude of the DLO can be predicted based on equation (7) if a whole period of the signal is obtained, but the vibrational amplitude cannot be derived directly with only a piece of signal segment. An alternative method is to calculate the vibration amplitude by;

$$A_s = \frac{A_{sl}}{A_{tl}} A_t \tag{21}$$

where A_s is the amplitude of the signal, A_{sl} and A_{tl} are the local amplitudes of the signal segment and the matched template segment, respectively, and A_t is the amplitude of the template. The distance of adjustment motion is determined (as discussed in Section 2.3 and 2.4) if A_s is acquired.

4. Implementation

For the sensor-based adjustment motion experiments, a Stäubli RX130 industrial robot was used. A standard 500mm stainless steel ruler with cross section of 0.5mm×18mm was used as the DLO in the experiment. One end of the ruler was grasped by pneumatic jaws, as shown in Figure 8, and the force/torque sensor was mounted on the wrist of the robot. The sensor used was an AdaptForce 50/100. The sensor weighs 0.35kg and its relative accuracy is 2% of full scale, the resolution (standard deviation of force sensor readings with filter 2) is F_x: 0.027N, F_y: 0.027N, F_z: 0.16N, M_x, M_y, and M_z : 0.0023Nm.

Figure 8. Experimental set-up. The DLO is grasped by pneumatic jaws and the robot conducts an adjustment motion to reduce vibration before inserting into a hole.

The experiments are conducted under various conditions with CCR- and MSE-based methods. First of all, the vibrational period and the stiffness coefficient δ of the DLO are measured off-line. In the following experiments samples were taken every

16ms. The damping coefficient β was set to 1. The internal system delay was neglected and t_{sys} is thus set to be zero. The two adjustment motions in two-way adjustment motion are conducted one immediately after another without overlapping or delay.

The overall on-line adjustment motion procedure consists of seven main steps, which are executed sequentially until the vibrational amplitude is smaller than a predefined threshold:

(1). The raw data from sensor is written into an array.
(2). The matching point is determined using template matching technique.
(3). The amplitude of the moment is computed.
(4). The direction of the adjustment motion is determined.
(5). The speed, acceleration and distance of the adjustment motion are determined.
(6). The adjustment motion is conducted.
(7). *The effects of the adjustment motion are evaluated.*

5. Experiments and Results

To verify the presented methods, experiments were conducted with different situations and methods; for example, in the horizontal plane, in the vertical plane and in the general plane, with the CCR method and the MSE method.

The speed of the robot jaw is defined by monitor speed and program speed [22]. In the following experiment, the monitor speed of the robot was set to 50% if not otherwise specified. The program speed altered automatically according to the scope of the adjustment motion and the vibrational period of the DLO. The program acceleration profile used was number 0 which is the strongest among the several types of acceleration profiles and was set to 100% [22] if not otherwise specified in the experiments.

5.1 Cases using CCR method

In this case, the DLO is grasped by pneumatic jaws with dominant vibration occurring in the horizontal plane, as shown in Figure 8. To contain at least one peak, the samples should cover at least one-and-a-half vibrational periods of the DLO. Here, all samples had a duration of 1.5 periods.

The vibrational period of the DLO was experimentally determined to be T=0.667s (frequency 1.5Hz), the constant δ, which is defined in equation (7), was determined to be 200mm/Nm before experiments. The vibrational amplitudes and moments of the DLO were measured before and after the adjustment motion. The vibrations were recorded with a video camera and read carefully later (Figure 9 shows one of the video images). Experimental results are shown in Table 1, Figure 10 and Figure 11, respectively.

Please note that the data in table 1 are obtained based on the following equations;

$$u = \sum_{i=1}^{n} x_i \frac{1}{n} \tag{22}$$

and

$$\sigma^2 = \sum_{i=1}^{n} (x_i - u)^2 \frac{1}{n} \tag{23}$$

where u is the average value and x_i is the measured data. The same method will also be used in the following cases.

Table 1. Vibrational amplitudes before and after adjustment motion (using CCR).

TAMo	*average amplitude and variance for 10 samples*		*amplitude reduction in percentage*
	before adjustment	*after adjustment*	
one-way	**26.71cm** (σ^2 = 0.4049)	**2.97cm** (σ^2 = 0.8681)	**88.88%**
two-way	**28.25cm** (σ^2 = 0.2885)	**2.98cm** (σ^2 = 0.4816)	**89.45%**

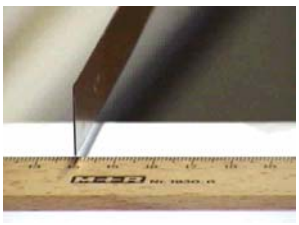

Figure 9. The endpoint vibration of the DLO along with a scaled ruler is recorded on video tape to be carefully read later.

As can be seen from Table 1, when the dominant vibration occurs in the horizontal plane, the amplitude of vibration was reduced from 26.71cm before adjustment to 2.97cm after application of the one-way adjustment motion. About 88.88%* of the vibrational amplitude was removed by the one-way adjustment motion. In the case of the two-way adjustment motion, the amplitude was reduced from 28.25cm to 2.98cm, a reduction of about 89%. It should be noted that the two-way adjustment motion has a smaller moving scope only one-half the one-way adjustment motion's.

The moment M_y corresponding to the dominant vibration occurring in the horizontal plane, and the results of FFT-analysis are shown in Figure 10 (one-way) and Figure 11 (two-way) respectively. Data cannot be recorded during the data processing period (from about 1.1s to 1.4s). It can be seen that the amplitudes of the moment were decreased with the use of a one- or two-way adjustment motion. The results of FFT-analysis also show the sharp decrease of **H**(f) corresponding to the dominant frequency after adjustment motions. Other low frequency vibrations, such as the second and the third mode vibrations, were not stimulated during the adjustment motion according to the FFT-analysis. Moreover, the presented method worked very well although the signals were not perfect Sine functions.

* Obtained by: (26.71-2.97)/26.71≈88.88%; the same method will be used in the following cases unless otherwise stated.

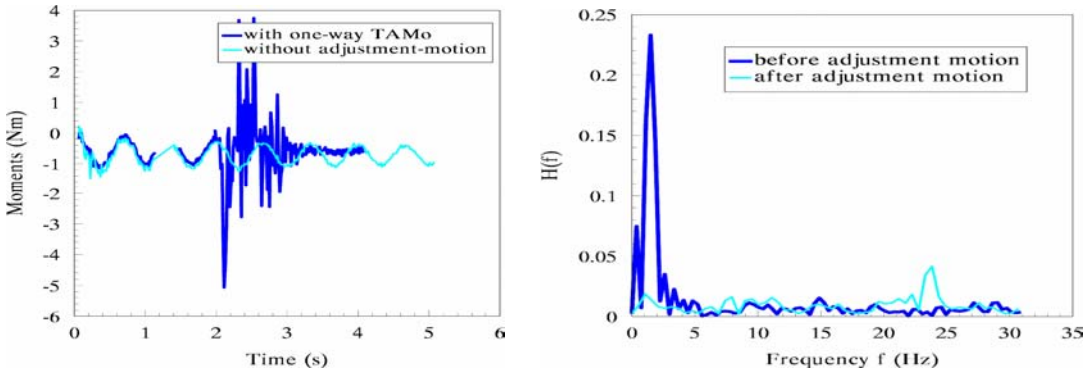

(a) (b)

Figure 10. (a). Dominant moment M_y during the one-way adjustment motion in which the CCR method is used, with dominant vibration occurring in the horizontal plane. (b). FFT-analysis of the DLO's vibration before and after adjustment motion.

As described in Table 1, Figure 10 and Figure 11, one-way adjustment motion can reduce the amplitude to 2.97cm within only 3.0 seconds. However, decline damped to the same level needs about 33 seconds according to our test. The two-way adjustment motion decreased the amplitude to 2.98cm within only 3.0 seconds, and decline damped to the same level costs about 34 seconds. So, the sensor-based adjustment motion is quite efficient.

It was noted that a high frequency around 24Hz in Figure 10(b) occurred during the adjustment motion. We recorded the data when the gripper conducted the same adjustment motion with and without DLO respectively. The FFT analysis shows the frequency around 24Hz was still there though not as obvious as before (Figure 12). In fact, not all the adjustment motions stimulate high frequency tremor according to our experiments. Compared with other low frequency residual vibrations, these kinds of high frequency tremors have almost no influence on the next operation.

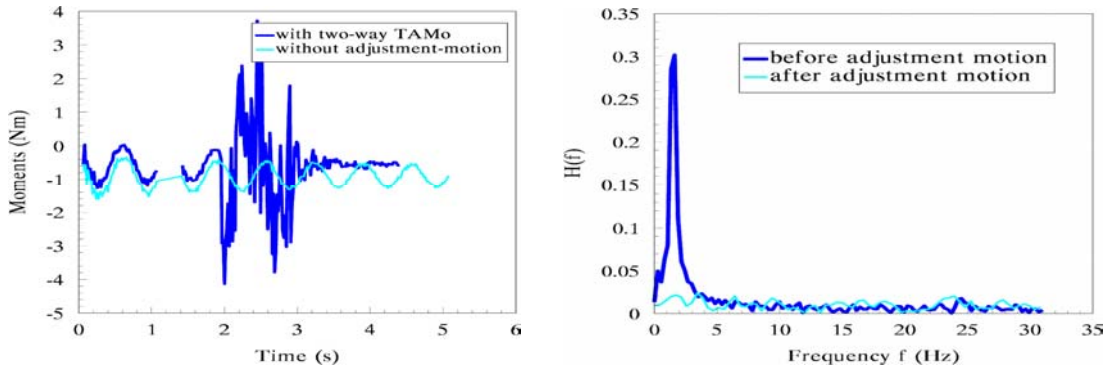

(a) (b)

Figure 11. (a). Dominant moment M_y during the two-way adjustment motion in which the CCR method is used, with dominant vibration occurring in the horizontal plane. (b). FFT-analysis of the DLO's vibration before and after adjustment motion.

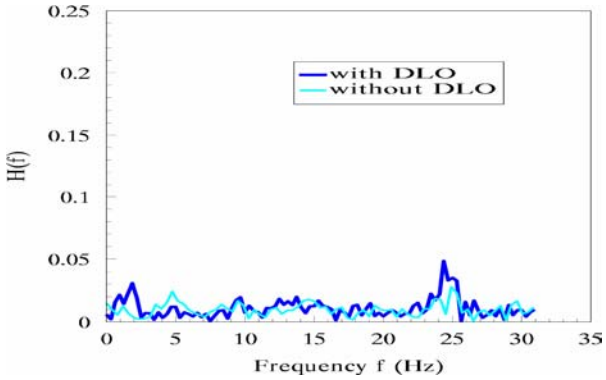

Figure 12. FFT-analysis of the data obtained when the gripper conducts the same adjustment motion with (bold line) and without DLO (thin line). The frequency around 24Hz is still there though slightly weaker without DLO. This frequency is probably coming from the robot system or system coupled with DLO and stimulated by fast motion. Its contribution to DLO's vibration amplitude is quite small.

Additional experiments were conducted with the same DLO at different frequencies. The frequency was changed to 1.15Hz in one of these experiments by sticking about 5g (two 50 pfennig coins) to the free end of the DLO. In this case, the amplitude decreased from 31cm to 3cm within 3.0 seconds with the same program as above, and the adjustment motion style was two-way TAMo. The recorded moments for this example during the adjustment motion process and the results of FFT-analysis can be found in Figure 13.

Although the results of the experiments proved the effectiveness of the presented methods, in practice it is possible to further reduce the sampling time using new methods like MSE. In the following sections, the MSE method is used to find the matching points to reduce the sampling time.

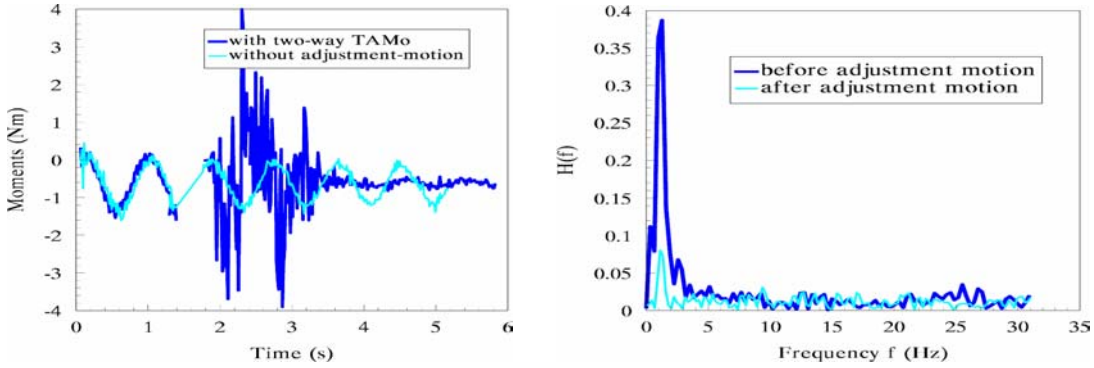

(a) (b)

Figure 13. Case of lower vibration frequency (1.15Hz) by addition of about 5g mass (two 50 pfennig coins) to the end of DLO. (a). the dominant moment M_y during the sensor-based two-way adjustment motion, with dominant vibration occurring in the horizontal plane. (b). FFT-analysis of the DLO's vibration before and after adjustment motion.

5.2 Cases using the MSE method

In this sub-section the MSE method is used to reduce the sampling time. It is expected that the new method can still find the matching point with few samples. However, the success probability in fact decreases with fewer samples from the sensor. Experiments were conducted to test the capability of the MSE method and results are shown in Figures 14 (a) and (b). It was found that with 20 samples (i.e. covering half a period), the MSE method can find the matching point with almost a 100% success rate. Thus, in the following experiments, samples covering half a period are used without further comment.

An increase in the number of samples increases the percentage of amplitude reduction, but the trend stops after 20 samples. In this situation (nearly one hundred percent success rates in finding the matching point), the main factor limiting the effects of adjustment motion is the resolution of the motion control.

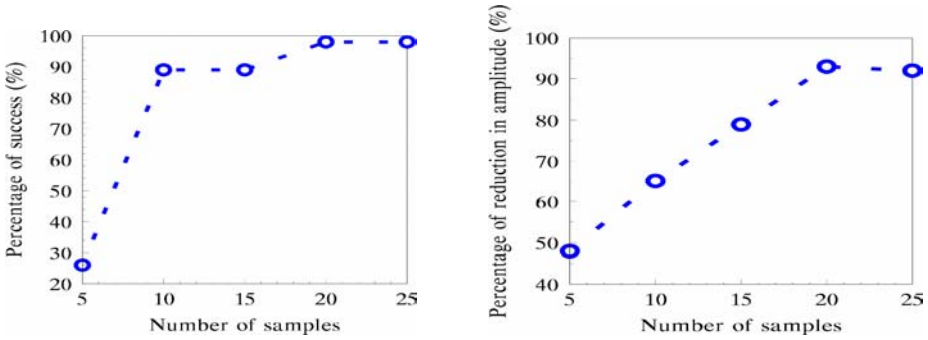

(a) (b)

Figure 14. Percentages of success and reduction versus number of samples used with MSE method. Samples here mean the sample from force/torque sensor every 16ms. (a) Success rates, where success in finding the correct match point is set to be 100% and the opposite phase is set to be 0; (b) The percentage of amplitude reduction after one-way TAMo. All the data are average values from 4 repeated experiments.

Table 2. Vibrational amplitudes before and after adjustment motion (using MSE).

TAMo	*average amplitude and variance for 10 samples*		*amplitude reduction in percentage*
	before adjustment	*after adjustment*	
one-way	**26.71cm** ($\sigma^2 = 0.4049$)	**2.83cm** ($\sigma^2 = 0.3121$)	**89.40%**
two-way	**26.71cm** ($\sigma^2 = 0.4049$)	**2.72cm** ($\sigma^2 = 0.6256$)	**89.82%**

As described in Table 2, Figure 15 and Figure 16, a one-way adjustment motion using MSE can decrease the amplitude to 2.72cm within only 2.3 seconds. The sampling time is decreased considerably compared with the CCR method. The two-way adjustment motion decreased the amplitude to 2.83cm within only 2.6 seconds, and sampling time is also quite reduced. Therefore, the MSE method is more efficient in finding the sensor-based adjustment.

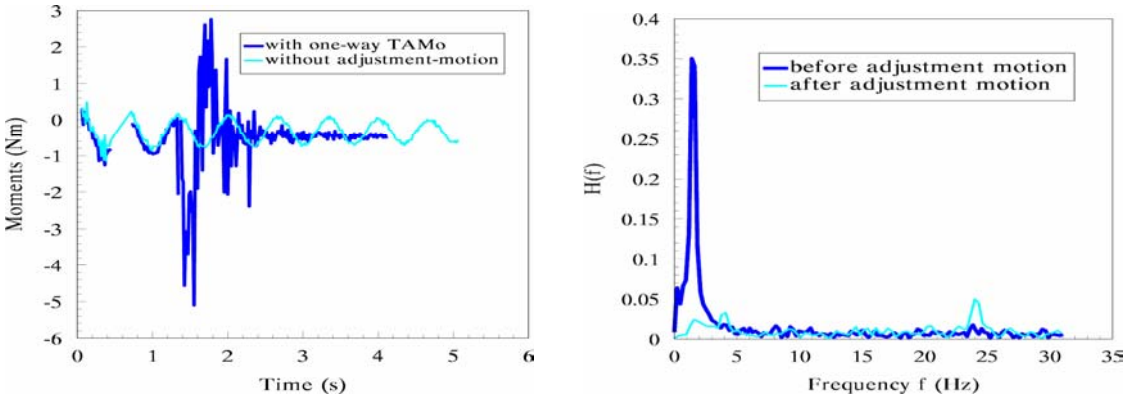

(a) (b)

Figure 15. (a). Dominant moment M_y during the one-way adjustment motion using the MSE method, with dominant vibration occurring in the horizontal plane. (b). FFT-analysis of the DLO's vibration before and after adjustment motion.

Additionally, to avoid collision, it is better to conduct the adjustment motion within the scope that the previous motion had just occupied. This means that the adjustment motion should start from an adjacent extreme with which collision is not possible. This criterion can be called the safe prior criterion (SPC). On the other hand, to reduce the waiting time, it is better to start adjustment motions as early as possible, no matter what kind of extremes (either maximum or minimum) are involved. This criterion can be called the wait-less criterion (WLC). Which demand can set the prior criterion depends on the environment and situations involved. For example, for two-way adjustment motions of very small scope, the safety may not be an important problem for this style of adjustment motion. Fortunately, sometimes these two demands can be satisfied at the same time, as shown in Figure 17. The adjustment motion starts from an adjacent valley and moves within the scope of previous motion. The total time required decreased to 2.1 seconds with a two-way TAMo.

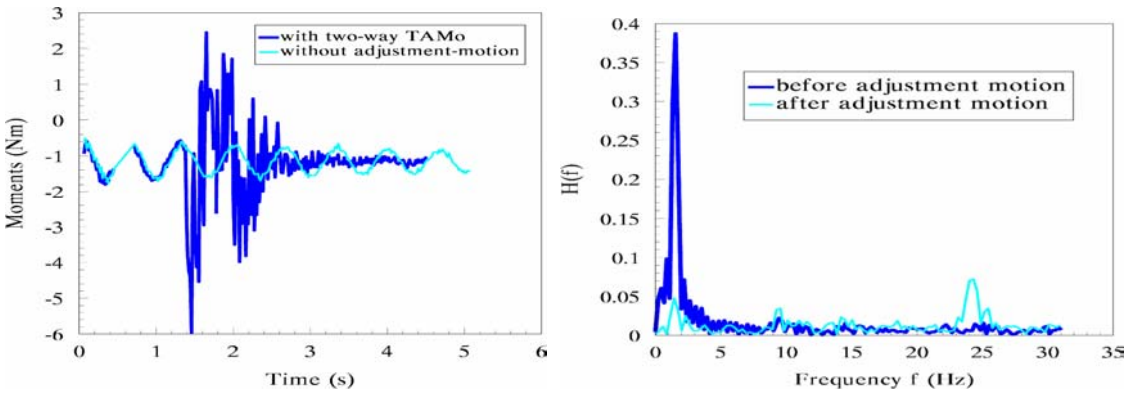

(a) (b)

Figure 16. (a). Dominant moment M_y during the two-way adjustment motion using the MSE method, with dominant vibration occurring in the horizontal plane. (b). FFT-analysis of the DLO's vibration before and after adjustment motion.

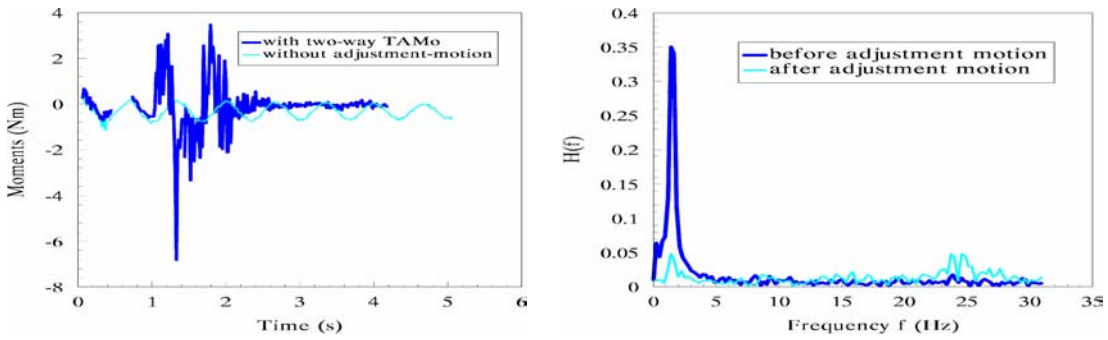

(a) (b)

Figure 17. The adjustment motion conducted within the scope of previous motion and dominant vibration occurring in the horizontal plane, safe prior criterion (SPC) and wait-less criterion (WLC) are satisfied in this case. (a). Dominant moment M_y during the two-way adjustment motion using the MSE method, (b). FFT-analysis of the DLO's vibration before and after adjustment motion.

5.3 Cases in vertical plane

Since the presented methods only depend on the amplitudes and phases of the signals, the large offset due to gravity will not affect the final results. Here we also present experiments in the vertical plane using our MSE method to find the matching point of the signals from the sensor. The adjustment motion is conducted with a safe prior criterion. The dominant vibration occurs in the vertical plane, and the DLO has a certain pre-deformation due to gravity. The measured dominant frequency changed slightly in the experiments and the period was 0.662 second. This period will be used in the following examples if not stated otherwise.

The results can be found in Table 3, Figure 18 and Figure 19. In the vertical plane with gravity, a one-way adjustment motion using MSE can decrease the amplitude to 2.81cm within only 1.5 seconds, reducing vibrational amplitude by 87.44%. The two-way adjustment motion can decrease the amplitude to 2.47cm within no more than 1.8 seconds, reducing vibrational amplitude by 88.96%. Therefore, the sensor-based adjustment motion has proven to be very efficient even with gravity.

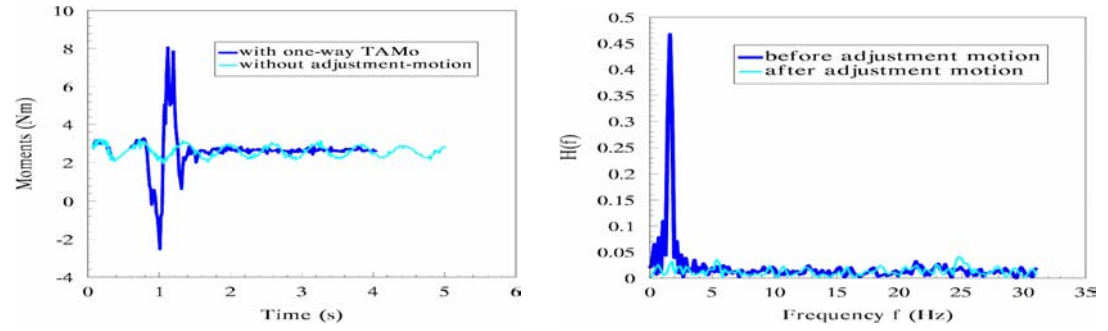

(a) (b)

Figure 18. Safe prior criterion (SPC) and wait-less criterion (WLC) were satisfied with dominant vibration occurring in the vertical plane. (a). Dominant moment M_y during the one-way adjustment motion using the MSE method; (b). FFT-analysis of the DLO's vibration before and after adjustment motion.

Table 3. Vibrational amplitudes before and after adjustment motion in the vertical plane (using MSE) with safe prior criterion (SPC) and wait-less criterion (WLC).

TAMo	*average amplitude and variance for 10 samples*		*amplitude reduction in percentage*
	before adjustment	*after adjustment*	
one-way	**22.37cm** ($\sigma^2 = 0.4241$)	**2.81cm** ($\sigma^2 = 0.6061$)	**87.44%**
two-way	**22.37cm** ($\sigma^2 = 0.4241$)	**2.47cm** ($\sigma^2 = 0.6961$)	**88.96%**

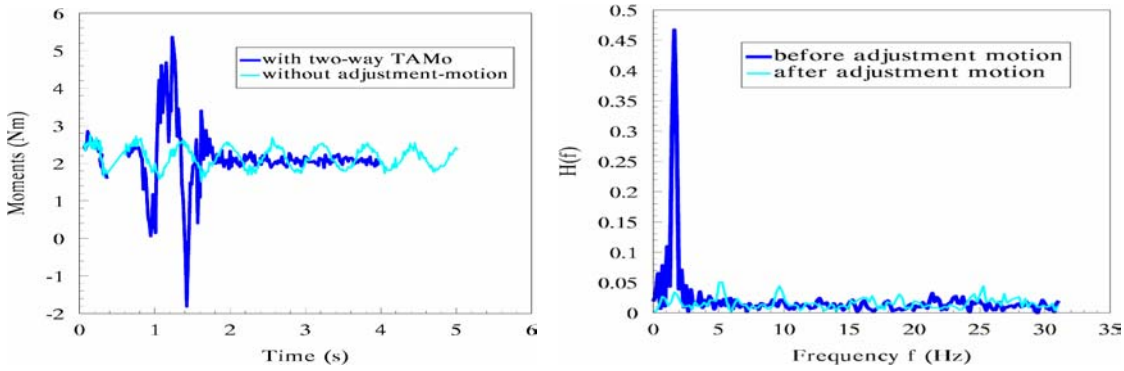

(a) (b)

Figure 19. Two-way adjustment motion with dominant vibration occurring in the vertical plane, Safe prior criterion (SPC) and wait-less criterion (WLC) were satisfied. (a). Dominant moment M_y during the two-way adjustment motion using the MSE method; (b). FFT-analysis of the DLO's vibration before and after adjustment motion.

5.4 Cases in general plane

When DLOs are handled in a certain plane that is neither a horizontal nor vertical plane, how does the presented method perform in this general situation? Here we also perform experiments in general cases to test the presented method. Safe prior criterion (SPC) and wait-less criterion (WLC) are used in these cases. The adjustment motions start with the TOOL coordinates x: 1104.998mm, y: -24.004mm, z: 316.320mm, yaw: -6.639^o, pitch: 114.825^o and roll: 50.071^o. Adjustment motion results are shown in Table 4, Figure 20 and Figure 21, respectively. In both of the cases, vibrational amplitudes were reduced to lower level within 2 seconds.

Table 4. Vibrational amplitudes before and after adjustment motion in general cases (using MSE) with safe prior criterion (SPC) and wait-less criterion (WLC).

TAMo	*average amplitude and variance for 10 samples*		*amplitude reduction in percentage*
	before adjustment	*after adjustment*	
one-way	**21.68cm** ($\sigma^2 = 0.1442$)	**3.36cm** ($\sigma^2 = 0.9684$)	**84.50%**
two-way	**21.68cm** ($\sigma^2 = 0.1442$)	**2.55cm** ($\sigma^2 = 0.4685$)	**88.24%**

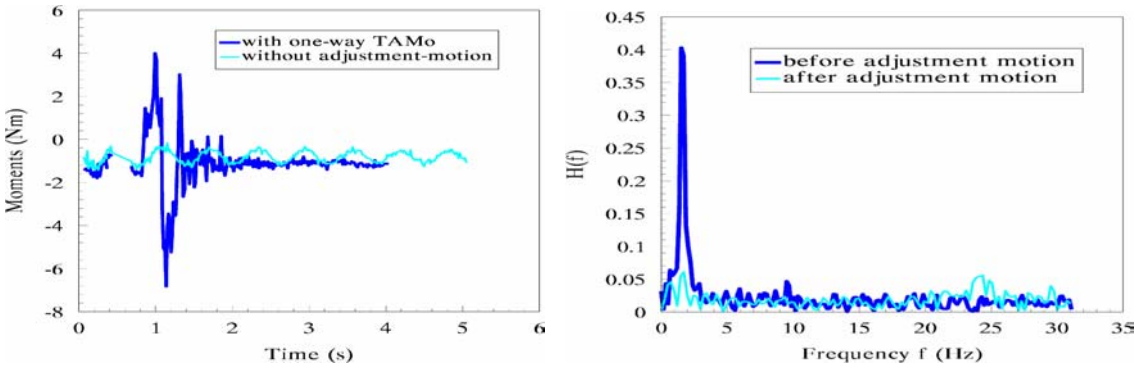

(a) (b)

Figure 20. One-way adjustment motion with dominant vibration occurring in the general plane, safe prior criterion (SPC) and wait-less criterion (WLC) were satisfied. (a). Dominant moment M_y during the one-way adjustment motion using the MSE method; (b). FFT-analysis of the DLO's vibration before and after adjustment motion.

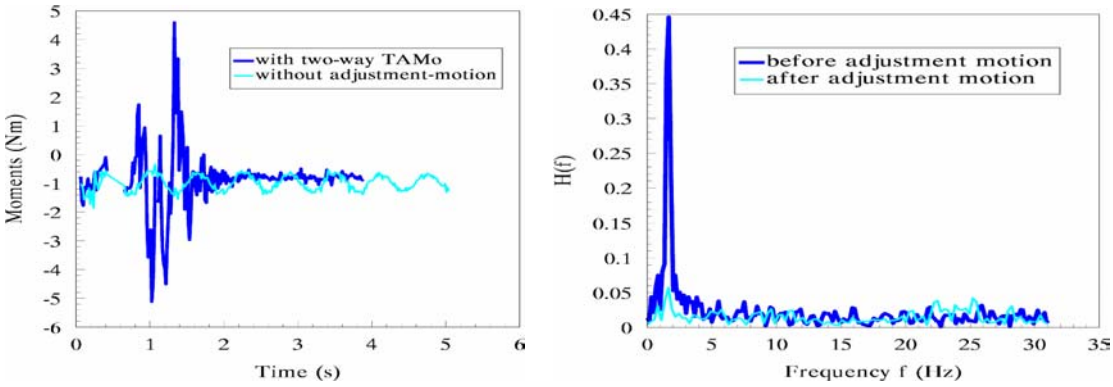

(a) (b)

Figure 21. Two-way adjustment motion using the MSE method with safe prior criterion (SPC) and wait-less criterion (WLC), dominant vibration occurring in the general plane. (a). Dominant moment M_y ; (b). FFT-analysis of the DLO's vibration before and after adjustment motion.

5.5 Effect of frequency errors

One may realize that errors in the off-line measured frequency could influence the vibration reduction. The problem here is just how much effect the frequency error actually has. For this reason, we investigated the effect of the presented method with respect to frequency errors experimentally. All of the experiments in this section were conducted under the same conditions (i.e. using the same algorithms and with dominant vibration occurring in the same horizontal plane, etc.) as in Section 5.2 except for variations in the frequencies. All of the values are the average of 4 samples

As shown in Figure 22, the percentage of amplitude reduction for one- and two-way adjustment motions decreases with increased error in the dominant frequency. However, for one-way adjustment motion, with errors within –2% to 2%, the adjustment motion can still reduce the vibrational amplitudes by more than 80%, as shown in Figure 22(a). Two-way adjustment motion with error between –4% to 2% can maintain a more than 75% reduction in vibrational amplitudes.

This implies that slight errors in the off-line measured frequency do not affect the presented methods very much. However, in most of the cases, effect of the vibration reduction will drop dramatically if error in dominant frequency is more than 2%.

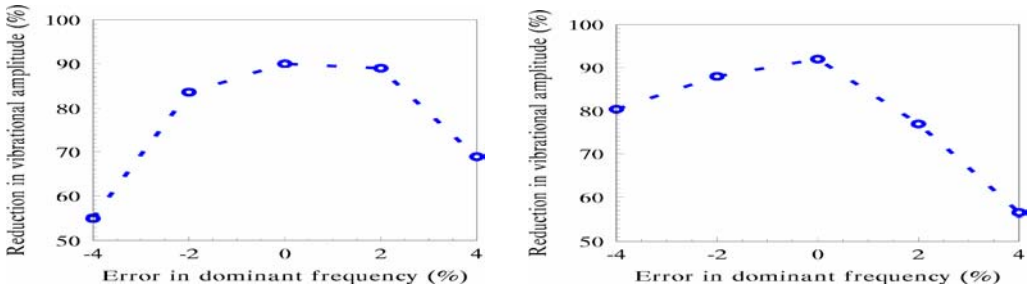

(a) (b)

Figure 22. The frequency errors can affect the reduction in vibration amplitude. Each point in the figures is averaged from 4 repeated experiments. (a) one-way adjustment motion, (b) two-way adjustment motion.

5.6 Summary and discussions of the experiments

In the above sections, several experiments have been done to test the sensor-based vibration reduction skills. We presented CCR and MSE methods to find the matching point in the experiments. The MSE method can achieve the same vibration reduction effect but saves about 1T in sampling. For almost each experiment, we provided one-way and two-way adjustment-motion respectively. The two-way adjustment-motion style is very convenient for the immediate execution of next operation, since the robot gripper will be back to its original position. Of course, a two-way adjustment-motion costs 0.5T more compared to a one-way one. The time required for a complete trial of adjustment motion with different matching point finding methods and criterions can be found in table 5.

Table 5. The time required for each method. The total time includes sampling, computing, waiting and execution time. Where T is the DLO's vibrational period.

Methods		Sampling	Computing	Waiting (at most)	Execution	Total time	Related Figures
CCR	One-way	1.5T	0.35s	0.75T	0.5T	2.75T+0.35s	Fig.10
	Two-way	1.5T	0.35s	0.75T	1T	3.25T+0.35s	Fig.11
MSE	One-way	0.5T	0.35s	0.75T	0.5T	1.75T+0.35s	Fig.15
	Two-way	0.5T	0.35s	0.75T	1T	2.25T+0.35s	Fig.16
	One-way (WLC)	0.5T	0.35s	0.5T	0.5T	1.5T+0.35s	Fig.18 and 20
	Two-way (WLC)	0.5T	0.35s	0.5T	1T	2T+0.35s	Fig.17,19 and 21

The total time of an adjustment motion is the added up time from sampling to the end of the execution of the adjustment motion. Using the CCR method, it costs at most (2.75T+0.35s) for one-way and (3.25T+0.35s) for two-way to finish a complete trial.

For the MSR method, it costs at most (1.75T+0.35s) for one-way and (2.25T+0.35s) for two-way respectively. Combining with a specified criterion, such as WLC which allows the adjustment motion to start from a nearest maximum/minimum, the total time required could be reduced to even shorter as listed in Table 5. However, the decline damps the same vibration to the same level costs tens of vibrational periods, for example, 34 seconds as mentioned in section 5.1.

Based on the results of the above experiments, the presented skills have been proven to be effective in practice. Although not all of the vibration can be eliminated due to the limited resolution of the robot system, it is reasonable to expect that if other low frequencies vibrations still behave dominantly, the sensor-based adjustment motion can also be used to reduce them in the same manner.

In the presented methods, we assumed that the robot's accelerating ability and the vibration period T satisfied

$$\frac{0.5T}{\Delta t} >> 1 \tag{24}$$

where Δt is the required time for the robot to accelerate its gripper to a certain high speed. There are several acceleration or deceleration profiles provided by the Robot supplier, we chose the fastest one as indicated in the experiment illustrations. It is clear that the presented method would be less effective or ineffective if the vibration frequency were much higher beyond the robot's motion abilities.

Additionally, internal system delay and variance of the robot acceleration are actually beyond our control during the experiment. However, as described in the moment figures above (sampling rate every 16ms), adjustment motion could always start at or tightly close to the expected time and slight delay has not affected the vibration reduction very much. The reason is probably because these perturbations are relatively weak and the skill is robust to these weak variations. For example, the system delay $t_{sys}<<0.25T$ as we have found in the above figures and described in [22]. On the one hand, could not control the acceleration in details makes the skill rather easy to be implemented; on the other hand, it is probably one of the reasons for the skills could not reduce the vibration to an even lower level, for example, from current centimeter level to millimeter level.

In the above experiments, we did not redesign the motion control law, which was already well developed by the suppliers. The only thing that an operator should do is to supply the robot with the vibrational period (or frequency) and the stiffness coefficient, which are measured off-line automatically with a well established program. In fact, this kind of calibration can also be performed on-line without significant difficulty, if demand for integration finally emerges.

As mentioned in section 3, vibration reduction skill could start from other point of time and other direction as well; DSA should be changed to cope with the new start point and direction. For example, start at the time when the DLO reaches its balanced position (where the deflection is zero for one DOF system), the DLO's vibration can be reduced too according to reference [23], in which the effect of a vibration reduction skill was tested with DLOs made of different materials and with different residual vibration amplitudes as well. The correlations between start time, directions and DSA might be

easy to establish and implement if skills are accommodated and/or mediated by an artificial neural network in the future.

7. Conclusions

In this article, special skills, i.e. force/torque sensor-based methods for eliminating acute vibration on-line during the handling of DLOs, were presented and the experimental results were discussed. Based on the simple strategies inspired from human skills, the attachable on-line skills can reduce the vibrational amplitude of DLOs effectively (cut by more than 85% on average) without stimulating other low frequency vibrations with an ordinary industrial robot.

Besides the strategies, most of the information to construct the skills is obtained from the force/torque sensor mounted on the robot's wrist. Unlike model-based methods, the sensor-based method does not use any information from previous motions. That is to say, the previous motion that resulted in vibration need not be known. The adjustment motion is generated automatically on-line by analyzing data from the sensor. Template matching technique and minimum squared error method are used to determine the matching point between the vibrational signal of the DLO and a template to meet different demands. Since the presented methods do not depend on the absolute value of signals from the sensor, they perform well whether or not there is an influence by gravity (which would result in offset of the absolute value).

These on-line skills are based on an open-loop concept without any feed-back information during operation. All the experiments were completed using an industrial robot. Therefore, the presented approaches could be easily used in practice due to their simple but effective characteristics. In the future, information from visual sensor may be integrated into the skill to simplify the implementation or extracted as redundant information to confirm the status of the DLO. Furthermore, to make the skill even more effective and flexible, neural networks with enough flexibility might be used.

Acknowledgments

The first author was a research fellow of the Alexander von Humboldt Foundation (AvH, http://www.avh.de). The Alexander von Humboldt Foundation is greatly appreciated by the first author. We thank Dr. Dirk EBERT, Mr. Antoine SCHLECHTER and Mr. Thorsten SCHMIDT for their very useful suggestions and help on sensor calibrating, video and digital picture capturing. We also thank Dr. Roger D. Santer and Dr. Richard Stafford who helped us check the English. We thank the anonymous reviewers for their comments which are very helpful in revising the paper.

References

[1] D. Henrich and H. Wörn (Editors), Robot manipulation of deformable objects, Springer, 2000, London, ISBN 1-85233-250-6

[2] M. Nakazawa, Handling of flexible object, TECHNO Japan, Vol.31, No.10, pp.30-35, Oct.1998
[3] Y.F. Zheng, R. Pei, and C. Chen, Strategies for automatic assembly of deformable objects, Proc. IEEE Int. Conf. On Robotics and Automation, pp.2598-2603, 1991.
[4] H. Wakamatsu, T. Matsumura, E. Arai and S. Hirai, Dynamic analysis of rod like object deformation towards their dynamic manipulation, Proc. of IEEE/IROS Int. Conf. On Intelligent Robots and Systems, pp.196-201, France, Sept. 1997
[5] S. Hirai, and H. Wakamatsu, Modeling of deformable strings with bend, twist, and extension in 3D space, Proc. 2nd ECPD int. Conf. On Advanced Robotics, Intelligent Automation and Active Systems, pp.529-534, Vienna, Sept. 1996.
[6] H. Inoue, M. Inaba, Hand-eye coordination in rope handling, Proc. of the First Int. Symp. on Robotics Research, pp. 163-174, New Hampshire, USA, Sept. 1983.
[7] P.W. Smith, N. Nandhakumar and A.K. Tamadorai, Vision based manipulation of non-rigid objects, Proc. IEEE Robotics and Automation, vol.4, pp.3191-3196, Minneapolis, Minnesota, USA, April, 1996
[8] W. Kraus, B. J. McCarragher, Case studies in the manipulation of flexible parts using a hybrid position/force approach, In: Proc. 1997 Int. Conf. on Robotics and Automation (ICRA'97), vol. 1, pp. 367372, Albuquerque, USA, April, 1997
[9] H, Nakagaki, K. Kitagaki, T. Ogasawara and H. Tsukune, Study of insertion task of a flexible beam into a hole by using visual tracking observed by stereo vision, Proc. of IEEE Int. Conf. On Robotics and Automation, Vol.4, pp.3209-3214, Minneapolis, USA, April, 1996
[10] J.D. Morrow, P.K. Khosla, Manipulation task primitives for composing robot skills, Proc. 1997 IEEE Int. Conf. on Robotics and Automation (ICRA'97), pp. 3354-3359, Albuquerque, USA, April 1997
[11] T. Hasegawa, T. Suehiro and T. Takase, A model-based manipulation system with skill-based execution, IEEE Trans. On Robotics and Automation, Vol.8, No.5, pp.535-544, 1992
[12] H. Onda, H. Hirukawa and K. Takase, Assembly motion teaching system using position/force simulator -extracting a sequence of contact state transition, Proc. of the IEEE/RSJ Int. Conf. On Intelligent Robots and Systems, Vol.1, pp.9-16, 1995
[13] D. Henrich, T. Ogasawara, and H. Wörn, Manipulating deformable linear objects – contact states and point contacts - , IEEE Int. Symposium on Assembly and Task Planning (ISATP'99), Porto, Portugal, July 21-24, 1999
[14] F. Abegg, A. Remde, and D. Henrich, Force and vision based detection of contact state transitions, '*Robot Manipulation of Deformable Objects*', Edited by Henrich D. and Wörn H., Springer, 2000, London, ISBN 1-85233-250-6.
[15] A. Remde, D. Henrich, and H. Wörn, Picking-up deformable linear objects with industrial robots, Int. Symposium on Robotics, Oct.27-29, 1999, Tokyo, Japan
[16] M.Z. Chen and Y.F. Zheng, Vibration-Free handling of deformable beams by robot end-effectors, J. of Robotics Systems, pp.331-347, 12(5), 1995
[17] J.F. Jones and B.J. Petterson, Oscillation damped movement of suspended objects, Proc. IEEE Int. Conf. On Robotics and Automation, pp.956-962, 1988
[18] G.P. Starr, Swing-free transport of suspended objects with a path-controlled robot manipulator, J. Dyn. System Control Trans. ASME, pp.97-100, 1985
[19] S.G. Yue and D. Henrich, Manipulating deformable linear objects: attachable adjustment motion for vibration reduction, Journal of Robot Systems, Vol.18(7), 2001, pp.375-389.
[20] MacCallion Henry, Vibration of linear mechanical systems, Longman, London, 1973

[21] R.O. Duda and P.E. Hart, Pattern classification and scene analysis, John Willy & Sons Inc. New York, 1973.
[22] Adept Techonology Inc. Adept V+ manual, 2000.
[23] Antoine Schlechter and Dominik Henrich, Manipulating deformable linear objects: maniuplatin skill for active damping of oscillations, IEEE International Conference on Intelligent Robots and Systems, Lausanne, Switzerland, September 20-Oct.4, 2002.